Вавиловский журнал генетики и селекции
Vavilov Journal of Genetics and Breeding. 2026;30(7):1035-1048

doi 10.18699/vjgb-26-105

Source-sink relationships governing grain yield in sodium azide-induced rice (*Oryza sativa* L.) mutants

Md Rezve [1], Md. Borhan Ali Sorker [2], Md. Musabbir Hossain Shoun [3], Md. Monirul Islam [1], S.M. Abdullah Al Mamun [1]

[1] Agrotechnology Discipline, Khulna University, Bangladesh
[2] Department of Agronomy, Sher-e-Bangla Agricultural University, Bangladesh
[3] Department of Biochemistry and Molecular Biology, Bangladesh Agricultural University, Bangladesh
mamun@at.ku.ac.bd

Abstract. Improving rice yield requires a clearer understanding of how source-sink relationships regulate productivity in mutation-derived germplasm. This study evaluated 101 genotypes, comprising 100 sodium azide-induced third-generation (M_3) rice mutants and their parental line, for 17 agronomic and yield-related traits under a randomized complete block design with three replications. Hierarchical clustering separated the population into two groups, and Cluster I showed superior performance for most productivity traits, including grain yield hill^{-1} (67.74 vs. 44.49 g), filled grains panicle^{-1} (144.85 vs. 118.62), straw yield hill^{-1} (86.19 vs. 71.04 g), and harvest index (44.21 vs. 39.04 %). Combining multivariate ordination with distributional statistics and correlation showed that there was considerable but continuous phenotypic variation within the mutants. Mixed linear model analysis with best linear unbiased prediction revealed very high broad-sense heritability for grain yield (0.97), straw yield (0.95), and harvest index (0.95), indicating strong genetic control. Sparse partial correlation analysis identified filled grains panicle^{-1}, straw yield hill^{-1}, and harvest index as the major directly associated traits of grain yield, with filled grains panicle^{-1} acting as the central hub in the trait network. Standardized regression ranked harvest index as the strongest predictor of yield, followed by straw yield and filled grain number. Response surface analysis revealed gradual nonlinear relationships among biomass production, sink strength, and harvest index with respect to underlying processes that are expected to influence source-sink interactions, rather than precise optimum states. These findings provide useful physiological and phenotypic insights for rice mutation breeding programs.

Key words: rice mutants; source-sink relationship; BLUP; graphical lasso; response surface analysis

For citation: Rezve Md, Borhan Ali Sorker Md., Musabbir Hossain Shoun Md., Monirul Islam Md., Abdullah Al Mamun S.M. Source-sink relationships governing grain yield in sodium azide-induced rice (*Oryza sativa* L.) mutants. *Vavilovskii Zhurnal Genetiki i Selektsii = Vavilov J Genet Breed*. 2026;30(7):1035-1048. doi 10.18699/vjgb-26-105

Data availability. The data that support the findings of this study are available from the corresponding author upon reasonable request.

Funding. We gratefully acknowledge the Research and Innovation Centre (RIC), Khulna University, for providing financial and institutional support essential for the successful completion of this research.

Взаимосвязи системы «источник–акцептор», определяющие урожайность зерна у мутантов риса (*Oryza sativa* L.), индуцированных азидом натрия

Мд Резве [1], Мд. Борхан Ал Соркер [2], Мд. Мусаббир Хоссейн Шоун [3], Мд. Монирул Ислам [1], С.М. Абдулла Аль Мамун [1]

[1] Кафедра агротехнологий, Университет Кхулны, Бангладеш
[2] Кафедра агрономии, Сельскохозяйственный университет Шер-э-Бангла, Бангладеш
[3] Кафедра биохимии и молекулярной биологии, Бангладешский сельскохозяйственный университет, Бангладеш
mamun@at.ku.ac.bd

Аннотация. Повышение урожайности риса требует более глубокого понимания того, каким образом взаимоотношения системы «источник–акцептор» регулируют продуктивность у генотипов, полученных в результате индуцированного мутагенеза. В настоящем исследовании был оценен 101 генотип (100 мутантов риса третьего поколения (M_3), индуцированных азидом натрия, и их родительская линия) по 17 агрономическим и связанным с урожайностью признакам в условиях рандомизированного полного блочного опыта с тремя повторностями. Иерархическая кластеризация разделила популяцию на две группы. При этом кластер I характеризовался более высокими значениями большинства признаков продуктивности, включая урожайность зерна с растения (67.74 против 44.49 г), число выполненных зерен в метелке (144.85 против 118.62), урожайность соломы с растения (86.19 против 71.04 г) и уборочный индекс (44.21 против 39.04 %). Комбинированный анализ с использова-

© Rezve Md, Borhan Ali Sorker Md., Musabbir Hossain Shoun Md., Monirul Islam Md., Abdullah Al Mamun S.M., 2026
This work is licensed under a Creative Commons Attribution 4.0 License

нием многомерной ординации, статистики распределения и корреляционного анализа показал наличие значительной, но непрерывной фенотипической изменчивости среди мутантов. С помощью анализа смешанной линейной модели с использованием метода наилучшего линейного несмещенного прогнозирования (BLUP) выявлена очень высокая наследуемость в широком смысле для урожайности зерна (0.97), урожайности соломы (0.95) и уборочного индекса (0.95), что свидетельствует о сильном генетическом контроле этих признаков. Анализ разреженных частных корреляций позволил идентифицировать число выполненных зерен в метелке, урожайность соломы с растения и уборочный индекс как признаки, наиболее непосредственно связанные с урожайностью зерна; при этом число выполненных зерен в метелке выступало центральным узлом сети признаков. Стандартизованный регрессионный анализ определил в качестве наиболее сильного предиктора урожайности уборочный индекс, за ним следовали урожайность соломы и число выполненных зерен. Анализ поверхности отклика выявил постепенные нелинейные взаимосвязи между накоплением биомассы, акцепторной способностью (sink strength) и уборочным индексом относительно процессов, которые, как предполагается, определяют функционирование системы «источник–акцептор», а не отражают строго определенные оптимальные состояния. Полученные результаты предоставляют важные физиологические и фенотипические сведения для программ селекции риса, основанных на использовании индуцированного мутагенеза.

Ключевые слова: мутанты риса; система «источник–акцептор»; BLUP; графическая лассо-регрессия; анализ поверхности отклика

Introduction

Rice (*Oryza sativa* L.) is the principal staple food for more than half of the global population and contributes substantially to daily caloric intake, especially in Asia. Sustaining rice productivity is therefore central to global food security. Population growth and increasing food demand necessitate continuous growth in rice production, but yield progress in many important rice-growing regions has slowed since the Green Revolution (Khush, 1999; Al-Hashimi, 2023; Bin Rahman, Zhang, 2023). This slowdown reflects the short genetic base of elite cultivars and decreasing returns from successive selection in relatively small breeding populations (Juma et al., 2021; Bhosale et al., 2025; Nalley et al., 2026). Expanding usable genetic variation has thus become a priority for future rice improvement.

Induced mutagenesis is an effective approach for creating novel heritable variation beyond that available in natural populations or conventional crosses. Sodium azide is especially useful among the chemical mutagens as it induces a high frequency of point mutations but it also has been found to cause substantially lower levels of chromosomal damage than much physical mutagen, thus allowing plants to survive and remain fertile (Raina et al., 2021; Türkoğlu et al., 2022; Mir, Jan, 2023). Worldwide, mutation breeding has made significant contributions to the improvement of crops and utilization of germplasm in nearly all cereal crops through the objective use of induced mutants to enhance yield, adaptability and quality traits (Ahloowalia et al., 2004; Kharkwal, 2023; Francis, Selvaraj, 2024). In rice, mutation-derived populations provide both superior lines for selection and a system for understanding how induced variation alters the determinants of yield.

Rice grain yield is a complex quantitative outcome controlled by multiple interdependent traits. Yield depends not only on sink size, such as grain number and panicle architecture, but also on source capacity, including biomass production and photosynthetic support, and on the efficiency with which assimilates are partitioned to developing grains (Anwar et al., 2022; Cheng et al., 2022; Vishwakarma et al., 2023; Hu et al., 2026). Traits like tiller number, panicle branching, filled grains panicle^{-1}, straw biomass and harvest index are physiologically related and can exhibit trade-offs or joint effects. This could result in selection based on mean performance alone or simple pairwise correlations being inadequate for isolating yield determinants from indirect associations caused by shared developmental processes or other confounding relationships (Begum et al., 2015; Rahman et al., 2024). This differentiation is essential because indirect traits have been shown to decrease the efficiency of selection and the physiological basis for enhanced performance in fast individuals may be hidden through improvement based on indirect traits.

Recent advances in quantitative analysis provide stronger tools for resolving these complexities. Best Linear Unbiased Prediction (BLUP) improves estimation of genotypic values and variance components by separating genetic effects from environmental noise, thereby strengthening heritability-based selection (Ahlinder et al., 2024; Piepho et al., 2024). Sparse partial correlation methods, including the Graphical Lasso, can identify conditional trait associations after removing indirect effects and are more informative than ordinary correlation analysis for detecting the independent drivers of yield variation (Ma et al., 2025; Kunst et al., 2026). Regression-based ranking and response surface analysis can further quantify the relative contribution of key variables and reveal nonlinear combinations of source and sink traits that associated with higher partitioning efficiency (Wang et al., 2026). Combined with clustering, distributional characterization, and multivariate association analyses, these methods provide an integrated framework for linking mutant-derived phenotypic variation with the physiological architecture of yield formation.

Although source-sink balance is an important factor underlying rice productivity, the vast majority of studies of mutation-derived rice germplasm have primarily examined variability estimates, mean comparisons and associations between traits. These strategies are informative for preliminary characterization but have limited information on the direct and indirect pathways leading to and through which traits regulate grain yield especially in chemically induced mutant populations where novel allelic combinations may be expected to perturb trait networks. Few studies have jointly integrated BLUP-based genetic evaluation, sparse partial correlation net-

works, multivariate association analysis, and response surface modeling to dissect source-sink relationships in sodium azide-induced rice mutants. Without identifying the independent yield-associated traits and their coordinated relationships, the breeding value of mutant populations cannot be fully exploited.

In this context, the present study investigated 100 sodium azide-induced M_3 rice mutants together with their parental genotype using 17 agronomic, yield, and yield-related traits. The objectives were to characterize phenotypic variability and population structure within the mutant population; to estimate the genetic control of key traits and identify the independent traits associated trait of grain yield; and to characterize coordinated source-sink trait relationships that may support selection in rice mutation breeding programs.

Materials and methods

Plant materials, study site, and experimental design. The experimental material comprised 101 rice genotypes, including 100 sodium azide-induced M_3 mutant lines and their parental genotype. The M_3 generation was selected for evaluation to assess the expression of induced variation after further advancement and stabilization of mutant phenotypes. The mutant population originated from sodium azide mutagenesis (Al Mamun et al., 2024) of the parental genotype (BRRI dhan28).

The experiment was carried out at the Experimental Farm of the Agrotechnology Discipline, Khulna University, Bangladesh, from July to October 2024. The study site is located at approximately 22°79′88″ E latitude and 89°53′44″ N longitude, with an elevation of about 18 m above sea level. The soil of the experimental field was clay loam in texture with a pH of 8.1. Soil analysis revealed an organic matter content of 5.38 % and total nitrogen of 0.222 %, along with available phosphorus of 16.36 μg g^{-1}, potassium of 0.34 mg 100 g^{-1}, sulfur of 31.40 μg g^{-1}, zinc of 2.88 μg g^{-1}, and boron of 1.23 μg g^{-1} (sample analyzed from Soil Resource Development Institute, Khulna). The climatic conditions prevailing during the experimental period are presented in Figure 1, based on records from the Regional Weather Station, Khulna.

The trial was laid out in a randomized complete block design (RCBD) with three replications. Each genotype was grown in a uniform plot arrangement (plot size = 3 m × 2 m; spacing = 25 cm × 25 cm), and standard agronomic practices for rice cultivation were applied uniformly throughout the growing season to minimize non-genetic variation. Observations were recorded from representative plants within each replication.

Trait measurement. Seventeen agronomic, yield, and yield-related traits were recorded following standard rice evaluation procedures. The phenological traits were days to flowering and days to maturity. Vegetative and plant architectural traits included plant height, total tillers $hill^{-1}$, effective tillers $hill^{-1}$, and flag leaf length. Panicle-related traits comprised panicle length, primary branches $panicle^{-1}$, and secondary branches $panicle^{-1}$. Grain and fertility traits included filled grains $panicle^{-1}$, sterile grains $panicle^{-1}$, grain length, grain breadth, and 1,000-grain weight. Productivity traits included grain yield $hill^{-1}$, straw yield $hill^{-1}$, and harvest index.

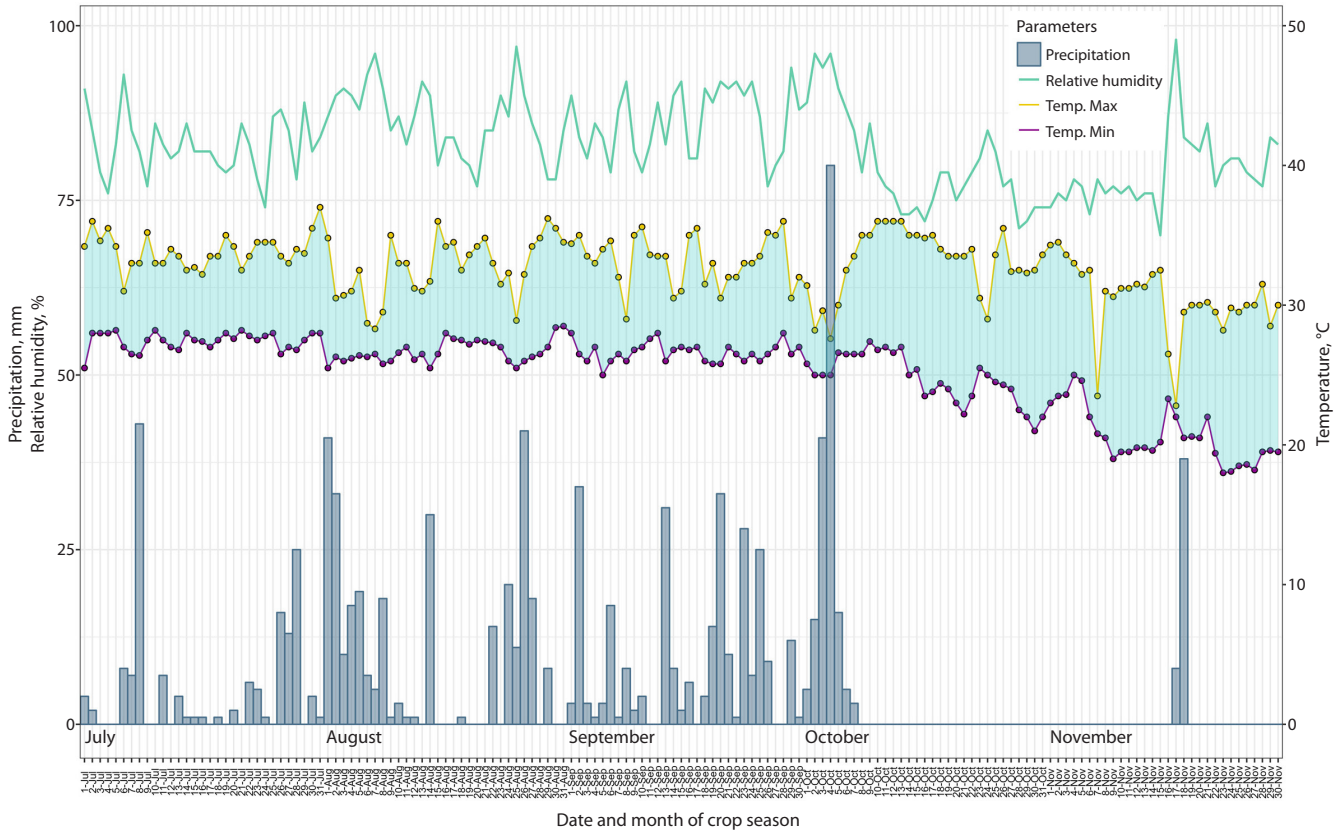


Fig. 1. Manifested weather situation during crop growing period.

Harvest index was calculated as:

$$\mathrm{HI}(\%) = \frac{\mathrm{GYH}}{\mathrm{GYH} + \mathrm{SYH}} \times 100.$$

Data preprocessing and standardization. To eliminate scale effects and ensure equal contribution of traits in multivariate analyses, trait values were standardized before analysis using the *z*-score transformation:

$$Z_{ij} = \frac{X_{ij} - \mu_j}{\sigma_j},$$

where Z_{ij} is the standardized value of trait j for genotype i, X_{ij} is the observed value, μ_j is the mean of trait j, and σ_j is the corresponding standard deviation.

Multivariate analysis of genotypic divergence and trait relationships. Genetic divergence among genotypes was first assessed by hierarchical cluster analysis using a quantitative dissimilarity matrix derived from standardized trait values. Euclidean distance between genotypes i and k was calculated as:

$$d_{ik} = \sqrt{\sum_{j=1}^{p} (Z_{ij} - Z_{kj})^2},$$

where p denotes the total number of traits. Genotypes were grouped using Ward's agglomerative clustering method to minimize within-cluster variance. Cluster-wise trait means were calculated on the original measurement scale.

To evaluate statistical differences between clusters, trait distributions were assessed using the Shapiro–Wilk normality test and Levene's test for homogeneity of variance. Depending on distributional characteristics, Student's t-test, Welch's t-test, or Mann–Whitney U test was applied. Statistical significance was determined at $p < 0.05$.

To further examine multivariate divergence, Mahalanobis D^2 distances were computed among genotypes as:

$$D^2_{ik} = (x_i - x_k)' S^{-1} (x_i - x_k),$$

where x_i and x_k are trait vectors for genotypes i and k, respectively, and S^{-1} is the inverse of the pooled variance-covariance matrix. The resulting distance matrix was subjected to principal coordinate analysis (PCoA) to visualize genotypic dispersion in reduced ordination space. Cluster-wise 95 % confidence ellipses were used to summarize within-cluster spread and between-cluster separation.

Pairwise relationships among traits were evaluated using Pearson's correlation coefficient:

$$r_{jk} = \frac{\sum (X_j - \overline{X}_j)(X_k - \overline{X}_k)}{\sqrt{\sum (X_j - \overline{X}_j)^2 \sum (X_k - \overline{X}_k)^2}}.$$

A trait-to-trait dissimilarity matrix was then generated using correlation distance $D_{jk} = 1 - r_{jk}$, and subjected to hierarchical clustering with Ward's linkage to identify coordinated trait modules related to phenology, vegetative growth, panicle architecture, and yield-biomass relationships.

Mixed linear model, BLUP estimation, and heritability. Variance components were estimated separately for each trait using a linear mixed model fitted under the RCBD:

$$y_{ij} = \mu + g_i + b_j + \varepsilon_{ij},$$

where y_{ij} is the observed value of genotype i in block j, μ is the overall mean, g_i is the random effect of genotype, b_j is the random effect of block (replication), and epsilon ε_{ij} is the residual error. The random terms were assumed to $g_i \sim N(0, \sigma^2_g)$, $b_j \sim N(0, \sigma^2_b)$, $\varepsilon_{ij} \sim N(0, \sigma^2_e)$.

Variance components were estimated by restricted maximum likelihood (REML), and genotype effects were predicted as Best Linear Unbiased Predictors (BLUPs).

Broad-sense heritability for each trait was calculated as:

$$h^2 = \frac{\sigma^2_g}{\sigma^2_g + \sigma^2_e},$$

where h^2 represents broad-sense heritability, σ^2_g is the genotypic variance, and σ^2_e is the residual variance.

Partial correlation analysis using Graphical Lasso. To identify conditional associations among traits after accounting for indirect relationships, partial correlation analysis was conducted on BLUP-adjusted trait values using the Graphical Lasso (GLASSO) approach (Friedman et al., 2008). The sparse precision matrix Theta was estimated by maximizing:

$$\log \det(\Theta) - \mathrm{trace}(S\Theta) - \lambda \| \Theta \|_1,$$

where S is the empirical covariance matrix, Θ is the precision matrix, and λ is the regularization parameter controlling sparsity. The optimal value of λ was selected using the Extended Bayesian Information Criterion (EBIC), and the model with the minimum EBIC value was retained.

Partial correlations were then obtained as:

$$\rho_{ij} = \frac{\Theta_{ij}}{\sqrt{\Theta_{ii}\,\Theta_{jj}}}.$$

Only stable non-zero partial correlations were retained for interpretation. These associations were treated as conditional statistical relationships rather than causal effects.

Trait interaction network analysis. A trait interaction network was constructed from the retained partial correlations, with traits represented as nodes and conditional associations represented as edges. Network topology was summarized using degree centrality:

$$C_D(i) = \sum_j a_{ij},$$

where a_{ij} indicates the presence or absence of an edge between traits i and j. Traits with high degree centrality were considered network hubs with greater connectivity within the overall trait architecture.

Regression modeling and response surface analysis. Standardized multiple linear regression was used to quantify the relative contribution of agronomic traits to variation in grain yield hill^{-1}:

$$\mathrm{GYH} = \beta_0 + \sum_{i=1}^{p} \beta_i Z_i + \varepsilon,$$

where β_i represents the standardized regression coefficient of the i-th predictor. The absolute magnitudes of the standardized coefficients were used to rank trait importance after accounting for the effects of the other variables in the model.

To evaluate nonlinear source-sink interactions, a second-order polynomial regression model was fitted with harvest index as the response variable and straw yield hill^{-1} and filled grains panicle^{-1} as predictors:

$$\mathrm{HI} = \beta_0 + \beta_1 \mathrm{SYH} + \beta_2 \mathrm{FG} + \beta_3 \mathrm{SYH}^2 + \beta_4 \mathrm{FG}^2 + \beta_5 (\mathrm{SYH} \times \mathrm{FG}) + \varepsilon,$$

where β_0 is the intercept; β_1 and β_2 are linear effects; β_3 and β_4 are quadratic effects; β_5 is the interaction effect; and ε is the random error term. Parameters were estimated by ordinary least squares. Model adequacy was evaluated using the coefficient of determination (R^2), root mean square error (RMSE), and the statistical significance of the linear, quadratic, and interaction terms at $p < 0.05$. Three-dimensional response surfaces and contour plots were generated to identify the combinations of biomass production and sink capacity associated with comparatively higher harvest index values.

Distribution analysis and statistical characterization. To describe phenotypic dispersion and distributional behavior of the major agronomic and yield-related traits, probability density histograms were generated using probability density normalization, in which the total area of all histogram bars equals one rather than the sum of the bar heights. Kernel density estimates were superimposed to provide a smoothed representation of the underlying distribution. Distributional statistics including mean, standard deviation, coefficient of variation (CV), skewness, and kurtosis were calculated for each trait. The normality of trait distributions was assessed using the Shapiro–Wilk test, along with visual assessment of patterns in histogram density and kernel density estimates.

Software and reproducibility. R (v 4.5.2) and Python (v 3.14.3) statistical software and computational packages were used for multivariate analysis, mixed linear modeling, sparse network construction, regression analysis, and response surface visualization. All statistical analyses and visualizations were conducted using standard statistical computing workflows in R and Python, whereas the remaining analyses were conducted in a standard statistical computing environment.

Results

Population structure of the M_3 mutants

Substantial phenotypic variation was observed among the 100-sodium azide-induced M_3 rice mutants and the parental genotype across the 17 agronomic, yield, and yield-related traits evaluated. Hierarchical cluster analysis based on the quantitative dissimilarity matrix grouped the 101 genotypes into two major clusters (Fig. 2). Cluster I comprised 56 genotypes (55.45 %), including the parental line and 55 mutant lines, whereas Cluster II comprised 45 mutant lines (44.55 %) (Table 1). The grouping pattern indicated moderate phenotypic structuring of the evaluated materials into two partially differentiated phenotypic clusters.

Cluster-wise variation in agronomic and yield-related traits

Most agronomic traits and yield-related traits had significant differences as determined by statistical comparison between the two clusters (Table 2). Cluster I exhibited significantly

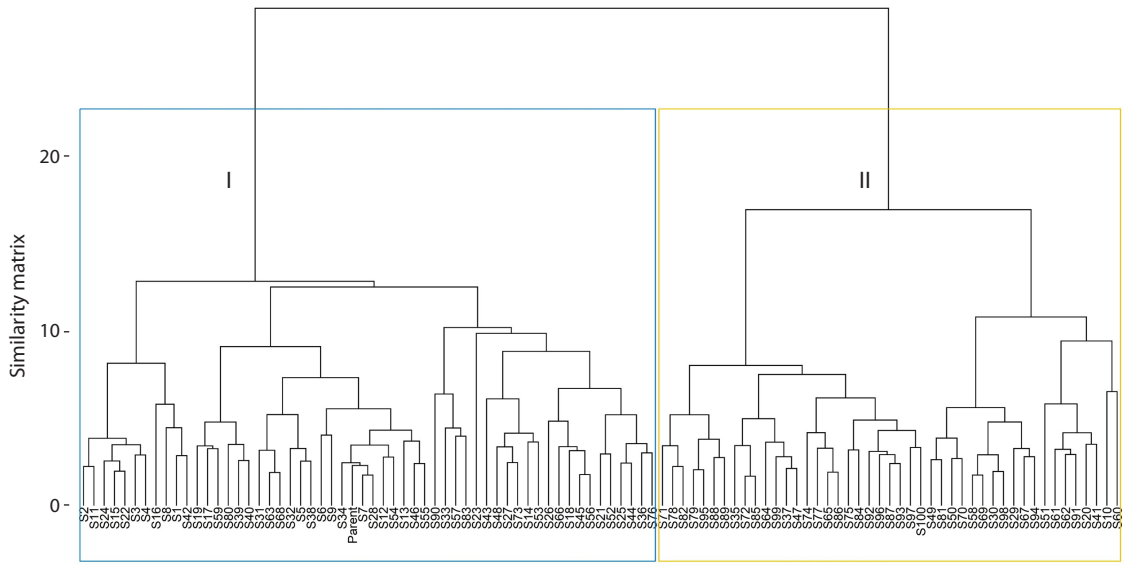


Fig. 2. Hierarchical cluster dendrogram based on the quantitative dissimilarity matrix showing the grouping pattern of the mutants (M_3) and their parent evaluated.

Table 1. Distribution of the rice genotypes in each cluster grouped by Ward's agglomerative clustering method

Cluster	Number of genotypes	Frequency, %	Name of genotypes
I	56	55.45	Parent, S1, S2, S3, S4, S5, S6, S7, S8, S9, S11, S12, S13, S14, S15, S16, S17, S18, S19, S21, S22, S23, S24, S25, S26, S27, S28, S31, S32, S33, S34, S36, S38, S39, S40, S42, S43, S44, S45, S46, S48, S52, S53, S54, S55, S56, S57, S59, S63, S66, S68, S73, S76, S80, S83, S90
II	45	44.55	S10, S20, S29, S30, S35, S37, S41, S47, S49, S50, S51, S58, S60, S61, S62, S64, S65, S67, S69, S70, S71, S72, S74, S75, S77, S78, S79, S81, S82, S84, S85, S86, S87, S88, S89, S91, S92, S93, S94, S95, S96, S97, S98, S99, S100

Table 2. Cluster-wise comparison of agronomic and yield-related traits with statistical significance

Trait	Cluster I	Cluster II	Statistical test	p-value	Significance
Days to flowering	84.60 ± 1.51	83.59 ± 1.49	Mann–Whitney U	<0.001	***
Days to maturity	120.60 ± 1.51	119.59 ± 1.49		<0.001	***
Plant height	87.72 ± 7.58	75.68 ± 8.13	Student t-test	<0.001	***
Tillers hill^{-1}	23.14 ± 4.35	21.61 ± 5.99	Mann–Whitney U	0.027	*
Effective tillers hill^{-1}	23.14 ± 8.73	20.87 ± 5.49		0.006	**
Panicle length	20.89 ± 1.74	19.23 ± 1.53		<0.001	***
Primary branches panicle^{-1}	9.62 ± 1.30	8.10 ± 1.34		<0.001	***
Secondary branches panicle^{-1}	21.85 ± 4.70	16.78 ± 4.46	Student t-test	<0.001	***
Flag leaf length	34.36 ± 5.15	27.84 ± 4.11	Mann–Whitney U	<0.001	***
Filled grains panicle^{-1}	142.01 ± 18.54	120.41 ± 17.67	Student t-test	<0.001	***
Sterile grains panicle^{-1}	13.61 ± 8.72	13.27 ± 7.57	Mann–Whitney U	0.905	NS
Grain length	9.31 ± 0.44	9.50 ± 0.45	Student t-test	<0.001	***
Grain breadth	2.49 ± 0.21	2.54 ± 0.18	Mann–Whitney U	0.061	NS
1,000-grain weight	18.10 ± 0.91	17.82 ± 0.79		0.004	**
Grain yield hill^{-1}	67.74 ± 13.93	44.49 ± 10.12		<0.001	***
Straw yield hill^{-1}	85.55 ± 12.34	70.82 ± 16.13		<0.001	***
Harvest index	44.00 ± 4.88	38.95 ± 7.29		<0.001	***

Note. Values are presented as mean ± standard deviation. Statistical significance between clusters was evaluated using Student's t-test, Welch's t-test, or Mann–Whitney U test depending on trait distribution characteristics. NS = non-significant; * $p < 0.05$; ** $p < 0.01$; *** $p < 0.001$.

higher mean values for grain yield hill^{-1}, straw yield hill^{-1}, harvest index, filled grains panicle^{-1}, panicle branching traits, flag leaf length, and plant height compared with Cluster II ($p < 0.05$). By contrast, the number of sterile grains panicle^{-1} and grain breadth were similar between the two groups.

Cluster II had a much higher value for grain length than Cluster I and most productivity-associated traits remained significantly superior in Cluster I, indicating moderate but significant phenotypic differentiation among the identified clusters rather than complete separation. Continuous phenotypic variation within the mutant population was evident from the substantial overlap among individual genotypes, despite significant differences for various traits.

Multivariate divergence revealed by principal coordinate analysis

Principal coordinate analysis (PCoA) based on Mahalanobis D^2 distances revealed moderate phenotypic structuring among the evaluated rice genotypes (Fig. 3). The cumulative variation explained by first two principal coordinates were 34.9 and 17.2 %, respectively amounting to 52.1 % of the total multivariate variation. The ordination pattern showed partial clustering tendencies between the two groups, although substantial overlap remained within the multivariate space, indicating incomplete separation among mutant-derived genotypes. The parental genotype was positioned within the broader ordination space occupied by the mutant population, indicating detectable but overlapping phenotypic divergence. However, shifts in overall trait composition between groups were detectable from displacement of cluster centroids. Additionally, based on the multivariate separation evidence shown by clustering analysis, this was also confirmed to be significant (Pseudo-F = 79.81, $R^2 = 0.446$, $p = 0.001$) with permutational multivariate analysis of variance (PERMANOVA). Thus, the ordination pattern is less consistent with strong multivariate differentiation than it is with partial separation of mutant-derived genotypes.

Variance components and BLUP-based heritability

The mixed linear model analysis revealed variation among traits in the relative magnitude of genotypic and residual variance components (Table 3). Grain yield hill^{-1} showed a genotypic variance of 278.22 and a residual variance of 8.16, resulting in a BLUP-based heritability estimate of 0.97. Straw yield hill^{-1} had a genotypic variance of 241.73 and a residual variance of 13.21, with heritability of 0.95. Harvest index also showed high heritability (0.95), with genotypic and residual variances of 41.22 and 1.98, respectively. Moderate heritability estimates were observed for filled grains panicle^{-1} (0.58), grain length (0.59), and 1,000-grain weight (0.61). Days to flowering and days to maturity each had heritability estimates of 0.73. Lower heritability estimates were recorded for effective tillers hill^{-1} (0.13), sterile grains panicle^{-1} (0.18), and primary branches panicle^{-1} (0.27).

Correlation-based grouping of agronomic and yield-related traits

Based on the hierarchical clustering of Pearson's correlation coefficients, the measured agronomic and yield-related traits formed several coordinated correlation modules (Fig. 4). Days to flowering and days to maturity showed significant positive association due to their related developmental regulation forming a tightly clustered phenological cluster. Grain morphol-

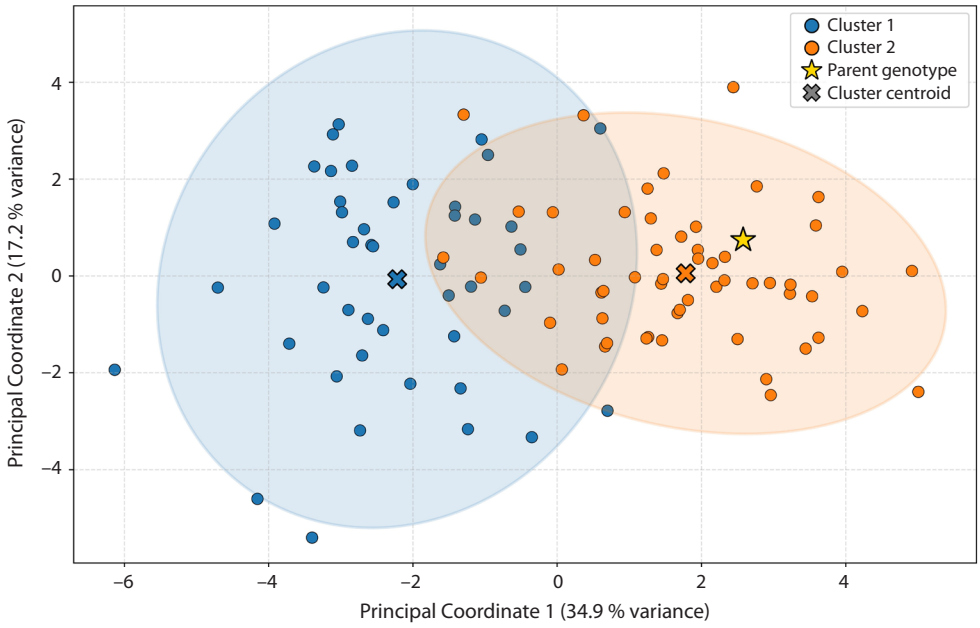


Fig. 3. Principal coordinate analysis (PCoA) showing partial multivariate differentiation among sodium azide-induced rice mutants and the parental genotype based on Mahalanobis D^2 distances.

Ellipses represent cluster dispersion within the ordination space, while centroid markers indicate the multivariate centers of the two clusters.

Table 3. Variance components and BLUP-based heritability estimate for agronomic traits in sodium azide-induced M_3 rice mutants

Trait	Genotypic variance (σ_g^2)	Residual variance (σ_e^2)	BLUP-based heritability (h^2)
Days to flowering	1.72	0.63	0.73
Days to maturity	1.72	0.63	0.73
Plant height	45.31	52.09	0.47
Tillers hill^{-1}	9.59	17.46	0.35
Effective tillers hill^{-1}	7.23	49.84	0.13
Panicle length	1.50	1.91	0.44
Primary branches panicle^{-1}	0.62	1.70	0.27
Secondary branches panicle^{-1}	12.34	15.19	0.45
Flag leaf length	11.84	20.68	0.36
Filled grains panicle^{-1}	258.93	187.31	0.58
Sterile grains panicle^{-1}	12.33	55.51	0.18
Grain length	0.10	0.07	0.59
Grain breadth	0.01	0.02	0.42
1,000-grain weight	0.43	0.28	0.61
Grain yield hill^{-1}	278.22	8.16	0.97
Straw yield hill^{-1}	241.73	13.21	0.95
Harvest index	41.22	1.98	0.95

ogy traits, including grain length and grain breadth, formed a relatively distinct trait cluster with comparatively weak associations with most productivity-related variables. Strong positive correlations existed among grain yield, harvest index, filled grain number, panicle branching traits and straw yield reflecting coordinated biomass production and sink strength towards higher yields. In contrast, several vegetative traits showed comparatively weaker or negative correlations with harvest index compared with grain yield and other panicle-related traits except for total tillers hill^{-1} and effective tillers hill^{-1}. Total tillers hill^{-1} and effective tillers hill^{-1} formed an additional subcluster reflecting their close developmental relationship and shared contribution to biomass accumulation. Observed correlation modules should not be interpreted as direct causal links between traits but rather coordinated statistical associations.

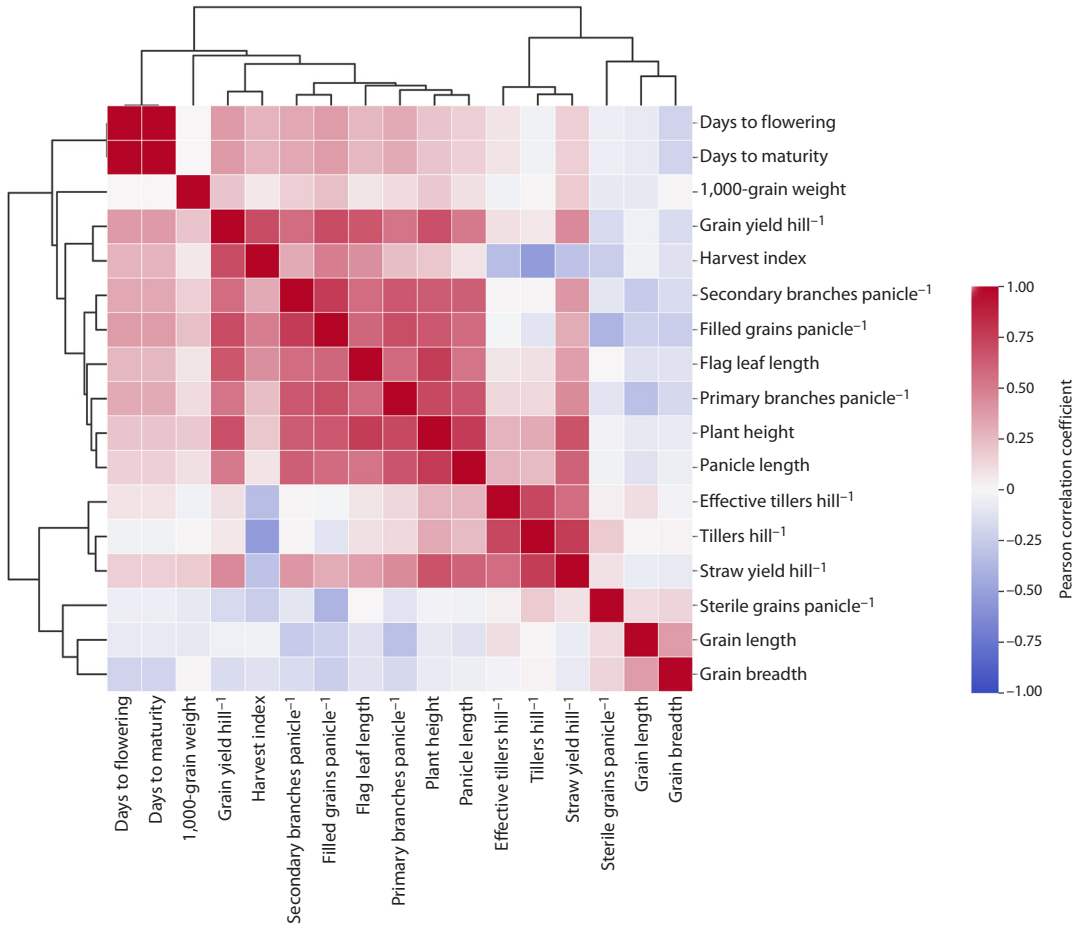


Fig. 4. Hierarchical correlation cluster map of agronomic, yield, biomass, and grain morphology traits in sodium azide-induced rice mutants.

The cluster map displays Pearson's correlation coefficients among measured traits after hierarchical clustering using Ward's linkage based on correlation distance. Red colors indicate positive correlations, whereas blue colors indicate negative correlations. The revised figure includes harvest index correlations and corrected grain morphology trait labels for improved interpretation of coordinated trait relationships.

Direct trait associations from BLUP-based partial correlation analysis

Partial correlation analysis based on BLUP-adjusted trait values and estimated using the Graphical Lasso produced a sparse pattern of direct conditional associations among the measured traits (Fig. 5). Days to flowering and days to maturity showed a strong positive conditional association. Total tillers hill^{-1} and effective tillers hill^{-1} were also directly and positively associated. Grain yield hill^{-1} showed positive partial correlations with filled grains panicle^{-1}, straw yield hill^{-1}, and harvest index. In contrast, grain yield hill^{-1} showed weak or negligible direct associations with grain size traits and most phenological variables. Harvest index and straw yield hill^{-1} showed a weak negative partial correlation.

Trait interaction network and node centrality

The trait interaction network constructed from significant BLUP-based partial correlations showed a sparse but structured topology (Fig. 6). Plant height, total tillers hill^{-1}, and filled grains panicle^{-1} appeared as the most connected nodes based on degree centrality. Filled grains panicle^{-1} showed direct positive links with secondary branches panicle^{-1}, effective tillers hill^{-1}, and grain yield hill^{-1}. Grain yield hill^{-1} was positioned between straw yield hill^{-1} and harvest index within the network structure.

Yield-associated predictors of traits to grain yield

The standardized multiple regression analysis identified differences in the relative contribution of traits to variation in grain yield hill^{-1} (Fig. 7). Harvest index showed the largest standardized effect, followed by straw yield hill^{-1}. Filled grains panicle^{-1} and secondary branches panicle^{-1} had moderate effects, whereas vegetative characters, grain morphology traits, and phenological traits contributed comparatively less in the fitted model.

Distribution of yield components, panicle architecture, and grain traits

Probability density histograms revealed broad phenotypic distributions for grain yield hill^{-1}, straw yield hill^{-1}, harvest index and filled grains panicle^{-1}, reflecting substantial variation in biomass production, sink strength and assimilate partitioning efficiency among the evaluated mutants (Fig. 8). Notably, panicle architecture traits such as primary branches panicle^{-1}

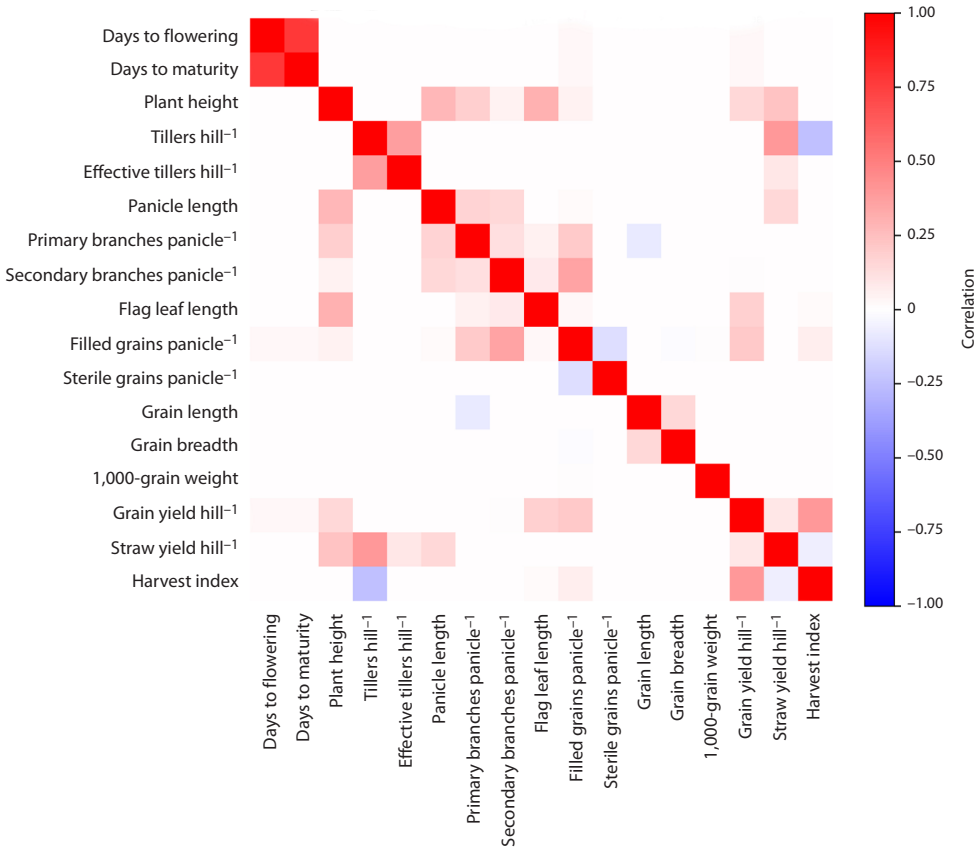


Fig. 5. BLUP-based partial correlation heatmap among agronomic traits estimated using the Graphical Lasso method.

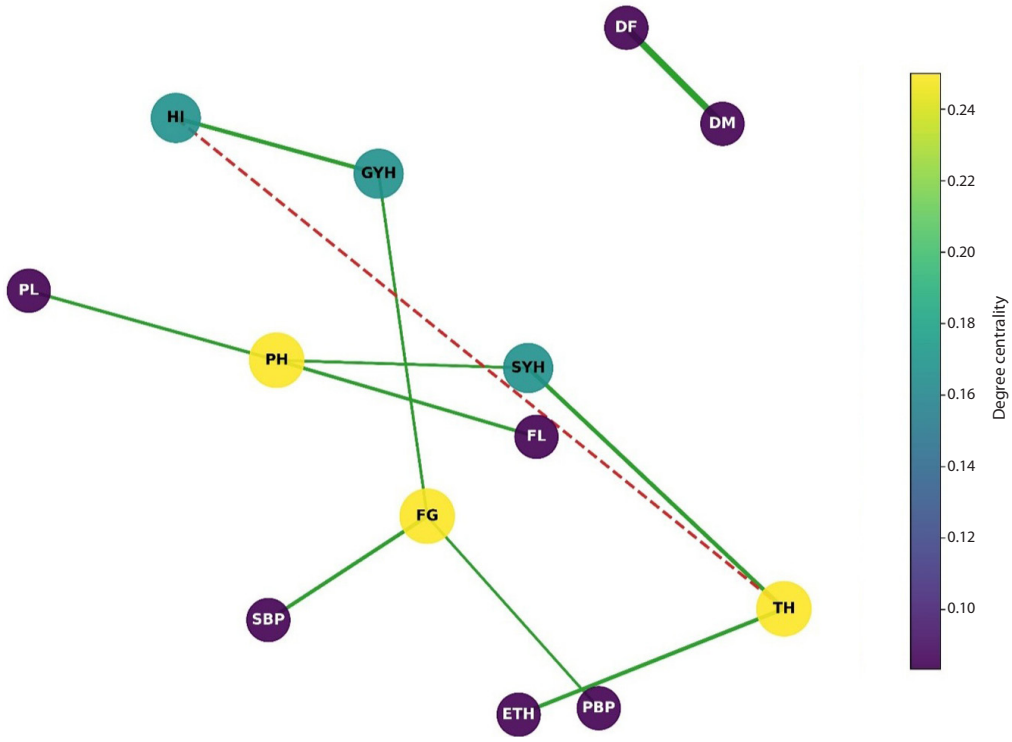


Fig. 6. Trait interaction network based on BLUP-derived partial correlations among agronomic and yield-related traits.

Here, DF = days to flowering; DM = days to maturity; PH = plant height; TH = total tillers hill^{-1}; ETH = effective tillers hill^{-1}; PL = panicle length; PBP = primary branches panicle^{-1}; SBP = secondary branches panicle^{-1}; FL = flag leaf length; FG = filled grains panicle^{-1}; GYH = grain yield hill^{-1}; SYH = straw yield hill^{-1}; HI = harvest index.

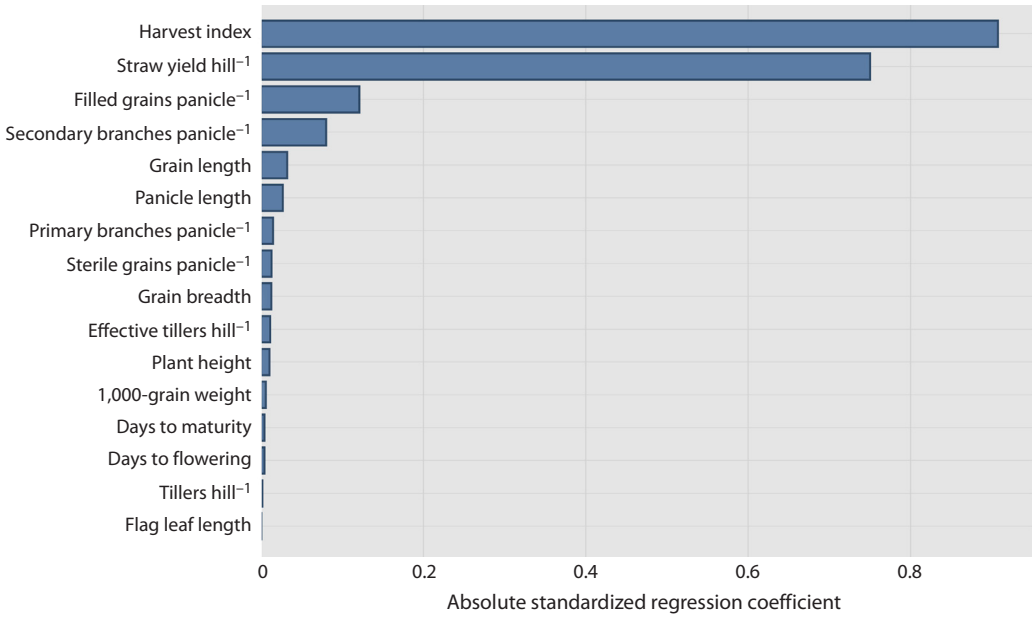


Fig. 7. Relative importance of agronomic traits for grain yield based on linear regression analysis.

Bar plot shows absolute standardized regression coefficients from a linear model fitted with grain yield hill^{-1} as the response variable. Larger values indicate stronger contributions of individual traits to yield variation after accounting for other predictors.

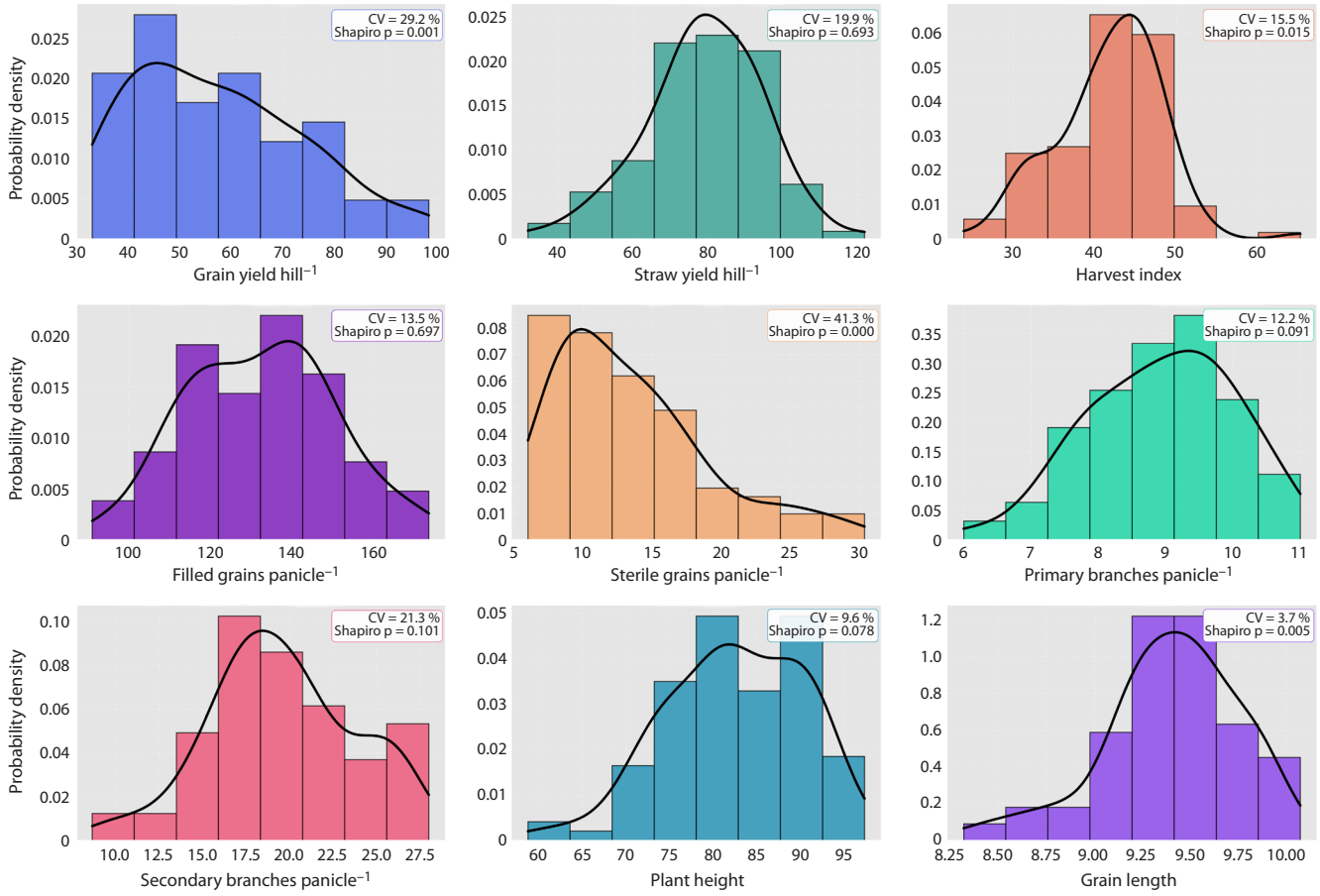


Fig. 8. Probability density histograms and kernel density estimate of major agronomic, yield, panicle architecture, and grain morphology traits in sodium azide-induced rice mutants.

Histogram densities and kernel density curves illustrate phenotypic dispersion and distributional behavior among evaluated genotypes. Embedded statistics indicate coefficient of variation (CV) and Shapiro–Wilk normality test results for each trait.

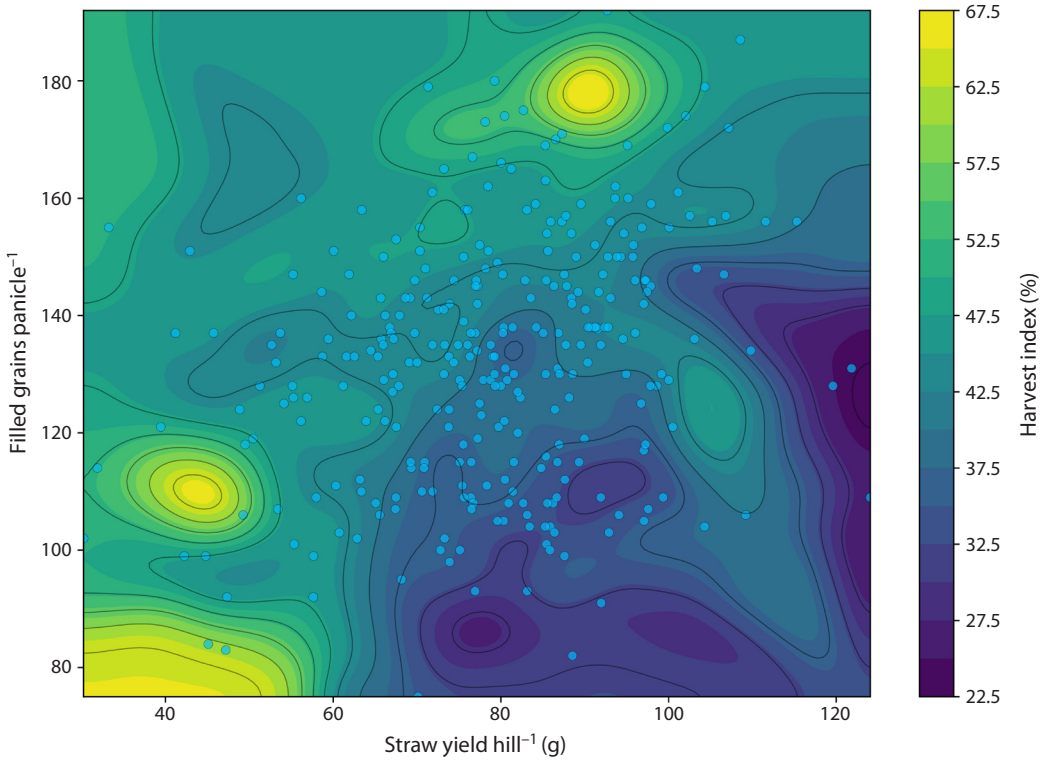


Fig. 9. Smoothed contour visualization illustrating the nonlinear association among straw yield hill^{-1}, filled grains panicle^{-1}, and harvest index.

The contour gradients indicate gradual variation in harvest index across the observed source–sink trait space. Comparatively higher harvest index values were generally associated with moderate biomass production combined with increased filled grain number. The figure is presented as a descriptive representation of source-sink relationships rather than a suggestive physiological optimization model.

and secondary branches panicle^{-1} also showed considerable phenotypic variation. Among the traits that were evaluated, sterile grains panicle^{-1} recorded the highest coefficient of variation (CV = 41.3 %) together with high positive skewness and a significant deviation from normality as per Shapiro–Wilk test ($p < 0.001$). The distributions of grain yield hill^{-1} and harvest index showed moderate departures from normality, while straw yield hill^{-1}, filled grains panicle^{-1}, primary and secondary branches panicle^{-1}, and plant height were close to approximately symmetric distributions with weaker or non-significant deviations. However, grain morphology traits such as grain length showed lower variability relative to other traits reflecting stable shape features across the mutant population.

Kernel density patterns further indicated substantial overlap among genotypes for some traits, demonstrating that despite the often-structured patterns observed in multivariate clustering analyses by which we identified genotypic groups, phenotypic variation for many traits is likely continuous. The measured overlap of density distributions gives further confidence in interpreting the mutant population as a phenotypic continuum, rather than completely discrete classes.

Response surface analysis of source-sink interaction

Response surface visualization demonstrated a gradual nonlinear association between straw yield hill^{-1}, filled grains panicle^{-1}, and harvest index across the observed trait space (Fig. 9). In general, comparatively high harvest index values were associated with moderate straw yield levels coupled with relatively higher filled grain number, while comparatively low harvest index values were indicated by lower sink strength and excessive biomass accumulation. Contour visualization showed smooth transitions across the source–sink trait space rather than discrete optimum regions. Given that harvest index is mathematically dependent on biomass partitioning, the trend in response observed here should be interpreted more as a descriptive mapping of source–sink relationships rather than a predictive physiological optimization model.

Discussion

The present study demonstrates that sodium azide mutagenesis generated substantial phenotypic variability across agronomic, productivity, and biomass-related traits within the evaluated rice population. Multivariate analyses suggested moderate phenotypic structuring among genotypes, although considerable overlap remained within the overall trait space. Hierarchical clustering grouped the 101 genotypes into two partially differentiated phenotypic groups, and there was significant multivariate differentiation between clusters (Pseudo-F = 79.81, $R_2 = 0.446$, $p = 0.001$; as determined with PERMANOVA). Nonetheless, the modest R^2 values and extensive distributional overlap observed for many traits suggest that the mutant population should be considered a phenotypic spectrum rather than

completely discrete groups. This interpretation is in agreement with the established quantitative basis of yield-related variation for rice, along with the gradual phenotypic alterations typically conferred by chemical mutagenesis (Türkoğlu et al., 2022; Mir, Jan, 2023). The comparatively higher grain yield, harvest index, filled grains panicle^{-1}, and biomass-related traits observed in Cluster I suggest that coordinated improvement in sink strength and assimilate partitioning contributed to superior productivity performance within part of the mutant population. In addition, similar phenotypic structuring in M_3 sodium azide-induced populations of rice has been reported previously which similarly recognized mutation-derived groups with contrasting combinations of yield and agronomic traits (Bordoloi et al., 2023; Al Mamun et al., 2024; Sofian, Purwanto, 2026).

The BLUP-based variance analysis provided important insights into the genetic control of productivity traits within this mutant population. The broad-sense heritability estimates (h^2) for grain yield, straw yield and harvest index were very high (0.97, 0.95 and 0.95, respectively), but comparatively lower h^2 estimation was reported for effective tillers hill^{-1} and sterile grains panicle^{-1} (0.13 & 0.18). Previous studies in rice breeding populations and mutation populations showed generally low heritability for yield and associated traits, indicating a strong environmental effect on final productivity (Riadi et al., 2018; Limbongan et al., 2024; Marlina, Syarif, 2025; Modarresi, 2026). The significantly higher heritability estimates seen in this present M_3 mutant population imply that the induced genomic variation for productivity traits was being expressed strongly and consistently with respect to the test environment; previous observations of reduced residual segregation and environmental sensitivity across generations of stabilization in rice mutant populations provide corroborating support (Oladosu et al., 2016; Viana et al., 2019). From a practical breeding perspective, the high heritability of grain yield, biomass production, and harvest index indicates that phenotypic selection for these traits may be comparatively effective within this mutant population under the evaluated environmental conditions. Conversely, the low heritability of effective tillers hill^{-1} signals that this component, despite its apparent contribution to yield, may be a less reliable target for direct phenotypic selection in similar mutant populations.

A particularly important contribution of the present study is the contrast between the ordinary correlation structure and the conditional associations revealed by the BLUP-based Graphical Lasso analysis. Conventional association studies in rice often identify many traits as correlated with yield, but such correlations may arise through indirect relationships and therefore provide limited guidance for efficient selection (Kumar et al., 2009; Spindel et al., 2015; Sassikumar et al., 2020). In the present analysis, only a small subset of traits retained direct associations with grain yield after indirect effects were accounted for, notably filled grains panicle^{-1}, straw yield hill^{-1}, and harvest index. These findings suggest that a comparatively smaller subset of traits remained conditionally associated with grain yield after indirect relationships were statistically accounted for.

The trait interaction network analysis further strengthens this interpretation by identifying filled grains panicle^{-1} appeared as one of the comparatively central traits linking several productivity-associated variables within the network structure. Grain number as one of the most important associated traits for rice yield potential has been suggested based upon decades of physiological and genetic studies (Casanova et al., 2002; Lu et al., 2022; Rahman et al., 2024), but the present work adds a more explicit network-level interpretation by showing that filled grains panicle^{-1} is not merely one component trait among many; it is structurally positioned at the connection of upstream architectural traits and final productivity. Thus, a relatively central location of filled grains panicle^{-1} among the determinants of several productivity-related traits across the mutant population evaluated is characterized by the network topology.

Despite its recognition that grain yield depends directly on source capacity, sink capacity and assimilate partitioning (Fukai et al., 1991; Tsukaguchi et al., 2016; Cheng et al., 2022; Vishwakarma et al., 2023; Hu et al., 2026), classical yield theory is often avoided in experimental studies where larger biomass or larger sink size is interpreted as inherently favorable (Lubis et al., 2003; Gendua et al., 2009; Lafarge, Bueno, 2009). The present response surface visualization, constructed as a descriptive representation of nonlinear source-sink associations rather than a definitive optimization model, indicated gradual transitions across the source–sink trait space. Comparatively higher harvest index values were generally associated with moderate straw yield levels combined with relatively higher filled grain number, whereas comparatively higher biomass accumulation alone was not consistently associated with increased harvest index values across the evaluated genotypes. Because harvest index is mathematically dependent on biomass partitioning, the observed response surface trends should be interpreted cautiously as descriptive statistical patterns within the evaluated experimental conditions rather than as strict physiological optima. These observations nonetheless suggest that balanced coordination between source production and sink realization may contribute to improved assimilate partitioning efficiency, which is consistent with broader physiological evidence for source–sink co-limitation in rice yield formation (Anwar et al., 2022; Hu et al., 2026).

The central role of harvest index in the current dataset is further supported by historical evidence. Previous studies showed that changes in harvest index was an important cause of cereal yield increases during the Green Revolution with improved varieties partitioning an increased fraction of total biomass into grain (Sinclair, 1998; Khush, 1999; Reynolds et al., 1999). The subsequent stagnation in yield progress in many rice environments has been attributed partly to the difficulty of further increasing harvest index while simultaneously expanding total biomass, reflecting a basic compromise in biomass partitioning (Tsusaka, Otsuka, 2013; Bin Rahman, Zhang, 2023). As with the modern mutant population, harvest index

was again identified as having high standardized regression coefficient in association with superior grain yield but response surface results show that its expression is dependent on the simultaneous interaction of biomass accumulation and sink realization rather than either factor working independently. This result suggests that mutation breeding might open up new avenues, not just by the creation of genotypes with larger absolute biomass or sink size, but also through producing novel combinations of source production and partitioning behavior that convert photosynthate to grain more efficiently. Previous results are in line with so far unreported evidence showing that high sink capacity enhances nitrogen and dry matter accumulation and ultimately yield performance under source-abundant conditions (Cheng et al., 2022; Vishwakarma et al., 2023; Hu et al., 2026).

Overall, the current study provides a quantitative description of source–sink relationships in a sodium azide-induced M_3 rice mutant population. The integrated framework combining multivariate clustering, PERMANOVA, BLUP-based partial correlation analysis, trait-by-trait networks, standardized regression and contour-response surface visualization is a more informative basis to study the structure of traits than performing single association analyses on descriptive data alone (Ahloowalia et al., 2004; Oladosu et al., 2016; Viana et al., 2019; Awan et al., 2021). Though previous works on induced rice mutant populations have focused largely on variability estimates and comparisons of mean traits, the current work identifies with greater specificity the conditional and network-level structure that yields a yield within a mutation-derived population. However, some important limitations need to be considered. Realizable heritability estimates can vary greatly depending on the cultivated environments sampled, and the high heritability estimates may simply reflect homogeneous environmental conditions experienced in this evaluation over a single growing season, rather than population-wide genetic stability across environments. Many of the variables evaluated are biologically interrelated, and harvest index is defined mathematically as the ratio of components of biomass; therefore, the associations reported herein are best interpreted as descriptive statistical relationships under the experimental conditions evaluated. The identified combinations of traits will have to be tested in multi-environment trials and true validation, before they can be used more extensively in rice breeding.

Conclusion

The present study demonstrated that sodium azide-induced mutagenesis generated substantial phenotypic variability in rice across agronomic, biomass, and yield-related traits. Multivariate analyses suggested moderate phenotypic structuring together with considerable overlap among genotypes, indicating continuous quantitative variation within the mutant population. Grain yield was most strongly associated with harvest index, straw yield, and filled grains panicle^{-1}, highlighting the importance of coordinated source–sink relationships in productivity formation. Collectively, these analyses provide useful insights into trait relationships and phenotypic variability that may support selection strategies in rice mutation breeding programs.

References

Ahlinder J., Hall D., Suontama M., Sillanpää M.J. Principal component analysis revisited: fast multitrait genetic evaluations with smooth convergence. *G3 Genes Genomes Genet*. 2024;14(12):jkae228. doi 10.1093/g3journal/jkae228

Ahloowalia B.S., Maluszynski M., Nichterlein K. Global impact of mutation-derived varieties. *Euphytica*. 2004;135(2):187-204. doi 10.1023/B:EUPH.0000014914.85465.4f

Al Mamun S.A., Ivy N.A., Khan M.A., Rehana S., Sultana M.S., Adhikary S.K., Islam M.M. Genotype selection from azide-induced rice mutants using multitrait genotype–ideotype distance index (MGIDI): unveiling promising variants for yield improvement. *Adv Agric*. 2024;2024(1):5719580. doi 10.1155/2024/5719580

Al-Hashimi A.M. A review: growing rice in the controlled environments. *Biosci Biotechnol Res Asia*. 2023;20(1):13-28. doi 10.13005/bbra/3064

Anwar K., Joshi R., Morales A., Das G., Yin X., Anten N.P., Raghuvanshi S., Bahuguna R.N., Singh M.P., Singh R.K., van Zanten M. Genetic diversity reveals synergistic interaction between yield components could improve the sink size and yield in rice. *Food Energy Secur*. 2022;11(2):e334. doi 10.1002/fes3.334

Awan F., Sadia B., Altaf J., Habib M., Hameed K., Hussain S. Genetic variability through induced mutation. In: Genetic Variation. IntechOpen, 2021. doi 10.5772/intechopen.95027

Begum H., Spindel J.E., Lalusin A., Borromeo T., Gregorio G., Hernandez J., Virk P., Collard B., McCouch S.R. Genome-wide association mapping for yield and other agronomic traits in an elite breeding population of tropical rice (*Oryza sativa*). *PLoS One*. 2015;10(3):e0119873. doi 10.1371/journal.pone.0119873

Bhosale S., Thathapalli Prakash P., Kadaru S.B., Hussain W., Dixit S., Ali J., Platten J.D., Islam M.R., Singh V.K., Murori R., Ndayiragije A. Onerice breeding framework: an end-to-end system to develop better varieties faster. *Crop Sci*. 2025;65(3):e70087. doi 10.1002/csc2.70087

Bin Rahman A.R., Zhang J. Trends in rice research: 2030 and beyond. *Food Energy Secur*. 2023;12(2):e390. doi 10.1002/fes3.390

Bordoloi D., Sarma D., Sarma Barua N., Das B.K. Mutation induction in aromatic *Joha* rice of Assam for improvement of morpho-agronomic traits through M_1 to M_3 generation. *Int J Radiat Biol*. 2023;99(11):1760-1777. doi 10.1080/09553002.2023.2214197

Casanova D., Goudriaan J., Forner M.C., Withagen J.C. Rice yield prediction from yield components and limiting factors. *Eur J Agron*. 2002;17(1):41-61. doi 10.1016/S1161-0301(01)00137-X

Cheng F., Bin S., Iqbal A., He L., Wei S., Zheng H., Yuan P., Liang H., Ali I., Xie D., Yang X. High sink capacity improves rice grain yield by promoting nitrogen and dry matter accumulation. *Agronomy*. 2022;12(7):1688. doi 10.3390/agronomy12071688

Francis A.P., Selvaraj R. A comprehensive review on mutation breeding milestones in cereals: conventional to advanced molecular approaches to achieve sustainable goals in trait improvement. *Horizon*. 2024;11(1):641-653. doi 10.14719/pst.3015

Friedman J., Hastie T., Tibshirani R. Sparse inverse covariance estimation with the graphical lasso. *Biostatistics*. 2008;9(3):432-441. doi 10.1093/biostatistics/kxm045

Fukai S., Li L., Vizmonte P.T., Fischer K.S. Control of grain yield by sink capacity and assimilate supply in various rice (*Oryza sativa*) cultivars. *Exp Agric*. 1991;27(2):127-135. doi 10.1017/S0014479700018780

Gendua P.A., Yamamoto Y., Miyazaki A., Yoshida T., Wang Y. Responses of yielding ability, sink size and percentage of filled grains to the cultivation practices in a Chinese large-panicle-type rice cultivar, Yangdao 4. *Plant Prod Sci*. 2009;12(2):243-256. doi 10.1626/pps.12.243

Hu Q., Zhang J., Yao Y., Xu K., Huo Z., Li G. Regulation of source–sink carbon partitioning for improving rice yield. *Physiol Plant*. 2026;178(2):e70847. doi 10.1111/ppl.70847

Juma R.U., Bartholomé J., Thathapalli Prakash P., Hussain W., Platten J.D., Lopena V., Verdeprado H., Murori R., Ndayiragije A., Katiyar S.K., Islam M.R. Identification of an elite core panel as a key breeding resource to accelerate the rate of genetic improvement for irrigated rice. *Rice*. 2021;14(1):92. doi 10.1186/s12284-021-00533-5

Kharkwal M.C. History of plant mutation breeding and global impact of mutant varieties. In: Mutation Breeding for Sustainable Food Production and Climate Resilience. Singapore: Springer Nature Singapore, 2023;25-55. doi 10.1007/978-981-16-9720-3_2

Khush G.S. Green revolution: preparing for the 21st century. *Genome*. 1999;42(4):646-655. doi 10.1139/g99-044

Kumar A., Verulkar S., Dixit S., Chauhan B., Bernier J., Venuprasad R., Zhao D., Shrivastava M.N. Yield and yield-attributing traits of rice (*Oryza sativa* L.) under lowland drought and suitability of early vigor as a selection criterion. *Field Crops Res*. 2009;114(1):99-107. doi 10.1016/j.fcr.2009.07.010

Kunst J.F., Melsen K.A., Kruijer W., Crossa J., Maliepaard C., van Eeuwijk F.A., Peeters C.F. A latent factor approach to hyperspectral time series data for multivariate genomic prediction of grain yield in wheat. *arXiv*. 2026. doi 10.48550/arXiv.2601.05842

Lafarge T., Bueno C.S. Higher crop performance of rice hybrids than of elite inbreds in the tropics: 2. Does sink regulation, rather than sink size, play a major role? *Field Crops Res*. 2009;112(2-3):238-244. doi 10.1016/j.fcr.2009.03.007

Limbongan Y., Sjahril R., Pata'dungan A.M., Parari T.Y. Genetic performance, heritability, and correlation of traits in new plant type of rice lines for highland ecosystem. *Reprod Breed*. 2024;4(4):203-211. doi 10.1016/j.repbre.2024.08.002

Lu Y., Chuan M., Wang H., Chen R., Tao T., Zhou Y., Xu Y., Li P., Yao Y., Xu C., Yang Z. Genetic and molecular factors in determining grain number per panicle of rice. *Front Plant Sci*. 2022;13:964246. doi 10.3389/fpls.2022.964246

Lubis I., Shiraiwa T., Ohnishi M., Horie T., Inoue N. Contribution of sink and source sizes to yield variation among rice cultivars. *Plant Prod Sci*. 2003;6(2):119-125. doi 10.1626/pps.6.119

Ma Y., Sun M., Liang X., Zhang H., Xiang J., Zhao L., Fan X. Rice yield and nitrogen use efficiency under climate change: unraveling key drivers with least absolute shrinkage and selection operator regression. *Agronomy*. 2025;15(3):677. doi 10.3390/agronomy15030677

Marlina G., Syarif A. Genetic variability and heritability estimates in M_1–M_3 generations of Kuantan Singingi local rice (White Sage genotype) induced by gamma radiation. *J Hunan Univ Nat Sci*. 2025;52(8):25-35. doi 10.55463/issn.1674-2974.52.8.3

Mir S.H., Jan I. Sodium azide as a mutagen. In: Biotechnologies and Genetics in Plant Mutation Breeding. Apple Academic Press, 2023;89-121

Modarresi M. Genetic variability, heritability and genetic advance in Iranian local rice genotypes for yield, and some agronomic traits. *Reprod Breed*. 2026;6(1):9-20. doi 10.1016/j.repbre.2025.12.003

Nalley L.L., Tack J., Durand-Morat A., Pede V., Villanueva D. Linking genetic gains to food security outcomes: an assessment of IRRI's rice breeding efforts in the Philippines and Indonesia. *Food Secur*. 2026. doi 10.1007/s12571-025-01632-7

Oladosu Y., Rafii M.Y., Abdullah N., Hussin G., Ramli A., Rahim H.A., Miah G., Usman M. Principle and application of plant mutagenesis in crop improvement: a review. *Biotechnol Biotechnol Equip*. 2016;30(1):1-16. doi 10.1080/13102818.2015.1087333

Piepho H.P., Williams E., Prus M. Assessing the efficiency and heritability of blocked tree breeding trials. *Tree Genet Genomes*. 2024;20(5):33. doi 10.1007/s11295-024-01666-6

Rahman M.A., Al Mamun M.A., Islam M.R., Quddus M.R., Munna N.A., Azim M.A., Galib M.S., Iftekharuddaula K.M., Syed M.A. Identifying key determinants of rice yield potential through multiple statistical techniques. *J Bangladesh Agric Univ*. 2024;22(1):17-28. doi 10.5455/JBAU.174200

Raina A., Ansari S.B., Khursheed S., Wani M.R., Khan S., Bhat T.A. Mutagens, their types and mechanism of action with an emphasis on sodium azide and gamma radiations. In: Mutagenesis, Cytotoxicity and Crop Improvement. Cambridge Scholars Publishing, 2021;1-37

Reynolds M.P., Rajaram S., Sayre K.D. Physiological and genetic changes of irrigated wheat in the post-green revolution period and approaches for meeting projected global demand. *Crop Sci*. 1999;39(6):1611-1621. doi 10.2135/cropsci1999.3961611x

Riadi M., Sjahril R., Kasim N., Diarjo R.H. Heritability and path coefficient analysis for important characters of yield component related to grain yield in M_4 red rice mutant. *IOP Conf Ser Earth Environ Sci*. 2018;157(1):012050. doi 10.1088/1755-1315/157/1/012050

Sassikumar D., Venmuhil R., Vanniarajan C., Indiran R. Selection indices for improving the selection efficiency of rice genotypes using grain quality traits. *Electron J Plant Breed*. 2020;11(02):543-549. doi 10.37992/2020.1102.091

Sinclair T.R. Historical changes in harvest index and crop nitrogen accumulation. *Crop Sci*. 1998;38(3):638-643. doi 10.2135/cropsci1998.0011183X003800030002x

Sofian A., Purwanto E. Yield stability and adaptability of newly selected black rice mutant lines (*Oryza sativa*) across dry-season agroecosystems in Central Java, Indonesia. *Biodiversitas*. 2026;27(1). doi 10.13057/biodiv/d270103

Spindel J., Begum H., Akdemir D., Virk P., Collard B., Redona E., Atlin G., Jannink J.L., McCouch S.R. Genomic selection and association mapping in rice (*Oryza sativa*): effect of trait genetic architecture, training population composition, marker number and statistical model on accuracy of rice genomic selection in elite, tropical rice breeding lines. *PLoS Genet*. 2015;11(2):e1004982. doi 10.1371/journal.pgen.1004982

Tsukaguchi T., Murakami K., Michimoto T. A quantitative measure for assimilate partitioning efficiency in rice (*Oryza sativa* L.). *Field Crops Res*. 2016;198:122-130. doi 10.1016/j.fcr.2016.08.033

Tsusaka T.W., Otsuka K. The changing effects of agro-climate on cereal crop yields during the green revolution in India, 1972 to 2002. *J Sustainable Dev*. 2013;6(4):11. doi 10.5539/jsd.v6n4p11

Türkoğlu A., Tosun M., Haliloğlu K. Mutagenic effects of sodium azide on in vitro mutagenesis, polymorphism and genomic instability in wheat (*Triticum aestivum* L.). *Mol Biol Rep*. 2022;49(11):10165-10174. doi 10.1007/s11033-022-07896-y

Viana V.E., Pegoraro C., Busanello C., Costa de Oliveira A. Mutagenesis in rice: the basis for breeding a new super plant. *Front Plant Sci*. 2019;10:1326. doi 10.3389/fpls.2019.01326

Vishwakarma C., Krishna G.K., Kapoor R.T., Mathur K., Dalal M., Singh N.K., Mohapatra T., Chinnusamy V. Physiological analysis of source–sink relationship in rice genotypes with contrasting grain yields. *Plants*. 2023;13(1):62. doi 10.3390/plants13010062

Wang L., Jia S., Zhao J., Liang C., Zhang W. Estimation of canopy traits and yield in maize–soybean intercropping systems using UAV multispectral imagery and machine learning. *Agriculture*. 2026;16(4):487. doi 10.3390/agriculture16040487

Conflict of interest. The authors affirm that this work is their original research and is not under consideration for publication. In addition, no competing of interest is declared by all the authors.

Received April 12, 2026. Revised July 1, 2026. Accepted July 6, 2026.